# Reports

## Strain Accumulation in the Shumagin and Yakataga Seismic Gaps, Alaska

J. C. SAVAGE, M. LISOWSKI, W. H. PRESCOTT

**Strain accumulation during the 1980–85 interval has been measured by means of trilateration surveys in the Shumagin and Yakataga seismic gaps, which are the two regions identified as the most likely sites for the next great thrust earthquakes along the Alaska-Aleutian arc. No significant strain accumulation was detected in the Shumagin gap, but experience at similar subduction zones and simple models of the subduction process suggest that a measurable amount of strain should have accumulated. The most likely explanation of the observation is that subduction there is either aseismic or episodic. The strain accumulation measured in the Yakataga gap is consistent with that expected for the plate convergence rate, although the direction of maximum compression may suggest a somewhat more oblique convergence than expected.**

ALTHOUGH MOST OF THE ALASKA-Aleutian arc has ruptured in a sequence of great earthquakes since 1938 (Fig. 1), there remain three major gaps that have not failed since about 1900. We are concerned with the easternmost two of those gaps. The Shumagin gap (center of Fig. 1) appears to have ruptured in 1788, 1847, and possibly 1903 (*1*). The Yakataga gap (top of Fig. 1) is known to have ruptured in 1899 (*2*). Both gaps are thought to have the potential for generating great earthquakes in the near future (*3*). However, the present strain rate in the Shumagin gap is so low that, if the same rate obtained in the past, sufficient strain to cause a great earthquake in the Shumagin gap may not yet have accumulated.

The U.S. Geological Survey has measured strain accumulation in both the Shumagin and Yakataga seismic gaps since about 1980. The strain accumulation is deduced from biennial surveys of trilateration networks established in those gaps. In each survey the distances between geodetic stations 10 to 30 km apart are measured with a Geodolite, a precise electro-optical distance-measuring instrument. The refractivity correction is determined from endpoint pressure measurements and temperature and humidity profiles determined by flying an aircraft along the line at the time of ranging. The standard error in measuring a line of length $L$ is $\sigma = (a^2 + b^2L^2)^{1/2}$, where $a$ is 3 mm and $b$ is 0.2 part per million (ppm) (*4*). For a distance of 20 km the standard error is about 5 mm.

U.S. Geological Survey, Menlo Park, CA 94025.

We have chosen to characterize the deformation of each network by the average rate of strain accumulation. To calculate that rate we assume that the deformation is uniform across the network both in space and time. Then the average rate of extension of each line is related to the surface components of the strain-rate tensor by

$$L^{-1}dL/dt = \dot\epsilon_{11}\sin^2\theta + 2\dot\epsilon_{12}\sin\theta\cos\theta + \dot\epsilon_{22}\cos^2\theta \qquad (1)$$

where $L$ is the line length and $\theta$ is the line azimuth measured clockwise from the 2-axis. The 1- and 2-axes are taken parallel (east-northeast) and perpendicular (north-northwest), respectively, to the local strike of the Alaska-Aleutian arc. Because the plate interaction at both gaps involves essentially perpendicular convergence, the 2-axis closely coincides with the direction of motion of the Pacific plate relative to the North American plate. The value of $dL/dt$ for each line is estimated from the slope of the linear fit to the data in a plot of line length against time. For each network, we have 20 or so relations (one for each line measured) of the form of Eq. 1 that can be solved for the surface strain rates $\dot\epsilon_{ij}$. Rather than report the strain rates $\dot\epsilon_{11}$, $\dot\epsilon_{12}$, and $\dot\epsilon_{22}$, we have chosen to use the shear-strain rates $\dot\gamma_1 = \dot\epsilon_{11} - \dot\epsilon_{22}$ and $\dot\gamma_2 = 2\dot\epsilon_{12}$ and the areal dilation $\dot\Delta = \dot\epsilon_{11} + \dot\epsilon_{22}$. We prefer to use the shear rates $\dot\gamma_1$ and $\dot\gamma_2$ rather than the extensions $\dot\epsilon_{11}$ and $\dot\epsilon_{22}$ because the shear components are more precisely determined in our measurements (*5*).

The implications of the measured strain rates are best understood in terms of a simple model of subduction. Although a completely satisfactory model of deformation at a subduction zone has not been developed, the conventional model that involves stick slip on the main thrust zone (the eventual rupture surface) and steady aseismic slip on the remainder of the plate interface furnishes a basis for discussion. Subject to several simplifying assumptions, the surface deformation on the overthrust plate in this model should be the same as that produced by a cycle of virtual, normal slip on the main thrust zone at the rate of plate convergence, interrupted periodically by major thrust events that recover the accumulated strain (*6*). For perpendicular plate convergence, the only nonzero component of the surface strain rate tensor is $\dot\epsilon_{22}$, the extension in the direction of plate convergence. Then the shear and dilatation rates are $\dot\gamma_1 = -\dot\epsilon_{22}$, $\dot\gamma_2 = 0$, and $\dot\Delta = \dot\epsilon_{22}$. Because of the larger standard error associated with $\dot\Delta$, comparison of the measured value for $\dot\gamma_1$ with the predicted value for $\dot\epsilon_{22}$ is the most sensitive test of how well the observations fit the simple model of strain accumulation.

The trilateration network in the Shumagin gap extends 110 km seaward (S30°E) from the Alaska peninsula to the outermost of the Shumagin Islands. The 39-line net-

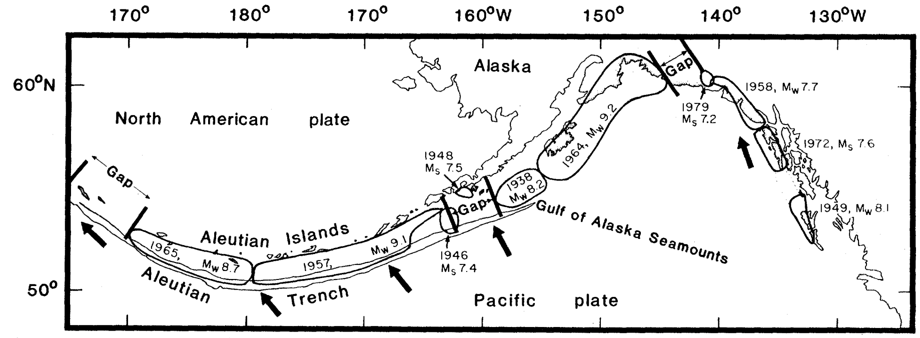


Fig. 1. Rupture areas of large, shallow earthquakes from 1930 to 1979 and seismic gaps along the Alaska-Aleutian arc. The Yakataga gap is marked at longitude 143°W and the Shumagin gap at longitude 160°W. The heavy arrows denote the direction of motion of the Pacific plate relative to the American plate [from (*15*)]. The magnitude scales $M_s$ and $M_w$ are described by Kanamori (*16*).

Table 1. Surface strain rates measured in the Shumagin and Yakataga seismic gaps. The 2-axis is oriented parallel to the direction of plate convergence (N30°W in the Shumagin gap and N15°W in the Yakataga gap), and the 1-axis is directed into the northeast quadrant. Extension is reckoned positive. The quoted uncertainties are standard errors.

| Network | Interval | $\dot{\gamma}_1 = \dot{\epsilon}_{11} - \dot{\epsilon}_{22}$ ($\mu$rad/year) | $\dot{\gamma}_2 = 2\dot{\epsilon}_{12}$ ($\mu$rad/year) | $\dot{\Delta} = \dot{\epsilon}_{11} + \dot{\epsilon}_{22}$ (ppm/year) |
|---|---|---|---|---|
| | | *Shumagin Islands* | | |
| All | 1980–85 | $-0.01 \pm 0.03$ | $-0.03 \pm 0.03$ | $-0.12 \pm 0.07$ |
| Inner | 1980–85 | $-0.01 \pm 0.03$ | $-0.02 \pm 0.03$ | $-0.12 \pm 0.07$ |
| Outer | 1981–85 | $0.03 \pm 0.05$ | $-0.05 \pm 0.06$ | $-0.20 \pm 0.10$ |
| | | *Yakataga* | | |
| All | 1979–84 | $0.26 \pm 0.05$ | $0.19 \pm 0.04$ | $-0.11 \pm 0.08$ |

work can be divided into two subnetworks: the 26-line inner islands network that extends 60 km seaward from the Alaska peninsula, and the 15-line outer islands network that extends an additional 50 km seaward. (Two lines are common to both subnetworks.) The inner island network was surveyed in 1980, 1981, 1983, and 1985, and the outer island network was surveyed in 1981, 1983, and 1985. The strain rates measured in the Shumagin Islands are shown in Table 1.

In the Shumagin gap, the Pacific plate converges on the American plate at the rate of about 75 mm/year in the direction N30°W (*7*), approximately perpendicular to the local strike of the Alaska-Aleutian arc. The main thrust zone dips 10° in the direction N30°W from the bottom of the Alaska-Aleutian Trench to the location of a sharp steepening (dip changes from 10° to 30°) of the plate interface just seaward of the outermost Shumagin Islands (*8*). The main thrust zone and the strain rate ($\dot{\epsilon}_{22} = -\dot{\gamma}_1$) profile for this model of subduction in the Shumagin gap are shown in Fig. 2. The predicted

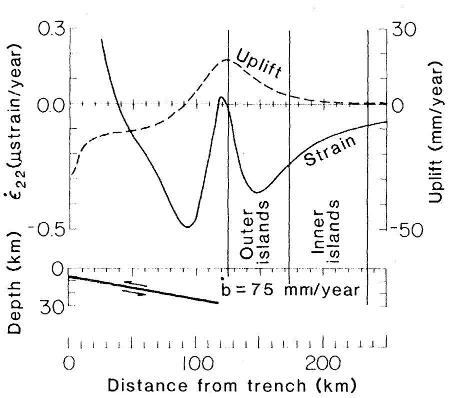


Fig. 2. Predicted strain rate (extension perpendicular to the strike of the subduction zone) and uplift rate profiles from south-southeast (left) to north-northwest (right) across the Shumagin subduction zone. The location of the main thrust zone in the model is shown in the lower sketch. The trilateration network spans the intervals designated as inner and outer islands.

value of $\dot{\gamma}_1$ is clearly significantly greater than the observed value (Table 1) for all cases (inner islands, outer islands, and entire network) in the 1980–85 interval.

Rather than compare the observed strain accumulation in the Shumagin gap with that predicted by a model of subduction, we compared it with the measured strain rates at another subduction zone. Along the east coast of Tohoku (northern end of the main island of Japan), the plate convergence rate is about a third larger than that at the Shumagin gap, but the strain networks in Tohoku are somewhat more distant from the main thrust zone than the Shumagin trilateration network. The observed extension parallel to the direction of plate convergence in Tohoku is about $-0.15$ $\mu$strain per year (*9*), implying a shear-strain rate $\dot{\gamma}_1$ of 0.15 $\mu$rad/year. Compared to this standard, the 1980–85 strain rates observed in the Shumagin gap (Table 1) are clearly deficient.

The absence of significant strain accumulation in the Shumagin network suggests the possibility of aseismic subduction (that is, subduction unaccompanied by great, shallow-thrust earthquakes). The argument against aseismic subduction is that great, shallow-thrust earthquakes have apparently occurred in the Shumagin gap in the past: two large earthquakes (presumably shallow-thrust events) occurred within 16 days of one another in 1788, both causing flooding (tsunami inundation) in the Shumagin Islands (*1*). Evidence for rupture of the gap in 1847 and 1903 is more equivocal. The current absence of shear-strain accumulation in the Shumagin gap implies a fundamental change in the character of slip on the main thrust zone: stick slip before the last great earthquake and stable sliding at present.

An alternative explanation for the absence of significant strain accumulation in the Shumagin gap may be that subduction there is episodic. This possibility is suggested principally by an episode of tilting in 1978–80 in the Shumagin Islands (*10*). That tilting was attributed to 1 m of aseismic slip on the segment of the plate interface immediately down-dip from the main thrust zone. Such a slip event would transfer the load formerly supported by the down-dip segment to the main thrust zone and consequently would appear as an episode of rapid strain accumulation. Thus, one could imagine long intervals in which strain accumulated very slowly, interrupted by occasional episodes of rapid accumulation. However, calculations suggest that even the minimum strain accumulation rate in such a model would be greater than the observed rate if the main thrust zone remained locked.

The trilateration network in the Yakataga gap extends about 60 km northward from the coast of the Gulf of Alaska at Cape Yakataga. The network consists of 19 lines surveyed in 1979–80, 1982, and 1984. (Twelve additional lines added in 1982 are not included in this discussion.) The strain rates measured in the Yakataga gap are shown in Table 1.

The Pacific plate converges on the American plate in the Yakataga gap at the rate of about 60 mm/year in the direction N15°W (*7*), roughly perpendicular to the extrapolated strike of the Alaska-Aleutian arc. However, the plate interaction at the Yakataga gap is not a simple subduction process but rather is complicated by the presence of the Yakutat block (or terrane), which is being carried on the Pacific plate into collision with the American plate (*11*). Nevertheless, to the extent that asthenosphere relaxation effects can be neglected, the simple elastic model of subduction can be applied to predict the interseismic deformation; the Yakutat block

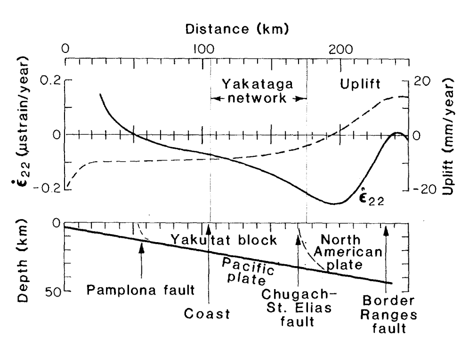


Fig. 3. Predicted strain rate (extension perpendicular to the strike of the subduction zone) and uplift rate profiles from south-southeast (left) to north-northwest (right) across the Yakataga subduction zone where the Pacific plate is being subducted beneath the North American plate. The Yakutat block is the wedge of material to the left of the Chugach–St. Elias fault and above the Pacific plate. The eventual rupture will not follow the Pacific plate interface to the free surface but rather will turn upward through the Yakutat block on one of the listric imbricate thrusts between the Chugach–St. Elias fault and the Pamplona fault zone.

rests on the Pacific plate (Fig. 3), and the interface between them plays the role of the main thrust zone (that is, there is no slip on the surface) during the strain accumulation interval. The ultimate rupture, however, does not follow that interface all the way to the trailing edge of the Yakutat block but rather breaks upward through the block (*12*) along one or more of the listric, imbricate thrust faults between the Pamplona fault zone and the Chugach–St. Elias fault (Fig. 3). A model for subduction and collision in the Yakataga gap and the associated strain rate ($\dot{\epsilon}_{22}$) profile is shown in Fig. 3. The down-dip end of the main thrust zone in that model is located at a change in dip in the plate interface inferred from seismicity (*13*). The model predicts a rate of strain accumulation across the Yakataga trilateration network with $\dot{\epsilon}_{22}$ equal to $-0.15$ μstrain per year and $\dot{\epsilon}_{11}$ and $\dot{\epsilon}_{12}$ both equal to zero. The equivalent shear strain rates are $\dot{\gamma}_1 = 0.15$ μrad/year and $\dot{\gamma}_2 = 0$. The observed value of $\dot{\gamma}_1$ ($0.26 \pm 0.05$ μrad/year) is somewhat larger than predicted but is within the range that could be accounted for by movement of the north end of the main thrust zone up-dip. The observed value of $\dot{\gamma}_2$ ($0.19 \pm 0.04$ μrad/year) indicates a right-lateral transverse shear not predicted by the model. This transverse shear may indicate that the plate convergence in the Yakataga gap is more oblique than suggested by the N15°W direction given by the model of Minster and Jordan (*7*). A more oblique convergence is supported by the coincidence between the N38°W direction of maximum compression and the N37°W strike of the Fairweather fault (locus of the 1958 rupture in Fig. 1), which is the right-slip transform that forms the lateral, North American—Pacific plate boundary in southeastern Alaska. This oblique convergence may be a product of slip-line flow (*14*) in which the Yakutat plate is squeezed to the west. In any case we are satisfied that strain is accumulating in the Yakataga gap at a rate commensurate with the eventual occurrence of a great plate-margin earthquake.


REFERENCES AND NOTES

1. J. Davies, L. Sykes, L. House, K. Jacob, *J. Geophys. Res.* **86**, 3821 (1981).
2. W. R. McCann, O. J. Pérez, L. R. Sykes, *Science* **207**, 1309 (1980). A small portion of the Yakataga gap did rupture in the 1979 St. Elias earthquake (Fig. 1) (see J. C. Lahr, C. D. Stephens, H. S. Hasegawa, J. Boatwright, *ibid.*, p. 1351).
3. K. H. Jacob, *Geophys. Res. Lett.* **11**, 295 (1984).
4. J. C. Savage and W. H. Prescott, *J. Geophys. Res.* **78**, 6001 (1973).
5. Systematic errors in trilateration tend to appear as proportional errors in line length (for example, all lines too short by 0.5 ppm). In calculating strain, such systematic errors are indistinguishable from an isotropic extension. Thus, a systematic error will appear directly in the tensor extensions $\epsilon_{11}$ and $\epsilon_{22}$ and in double proportion in the areal dilatation Δ. Because the shear components are the differences between two orthogonal extensions, those components are relatively free of proportional error. In our measurements, the error in measuring a line is composed of about equal parts random and systematic error. In calculating strain the random errors from the redundant observations tend to cancel, so that systematic error becomes dominant [see J. C. Savage, W. H. Prescott, M. Lisowski, N. E. King, *ibid.* **86**, 6991 (1981)].
6. J. C. Savage, *ibid.* **88**, 4984 (1983). A critical element in calculating the deformation rates is the particular earth model used. We have used an elastic half-space representation. That model yields the time-averaged deformation over the entire interseismic interval. A more complicated model that includes representation of a viscoelastic asthenosphere yields a time-dependent deformation in which the more rapid rates occur early in the cycle [see W. Thatcher and J. B. Rundle, *ibid.* **89**, 7631 (1984)].
7. J. B. Minster and T. H. Jordan, *ibid.* **83**, 5331 (1978).
8. M. Reyners and K. S. Coles, *ibid.* **87**, 356 (1983).
9. K. Nakane, *J. Geodetic Soc. Japan* **19**, 200 (1973).
10. J. Beavan, E. Hauksson, S. R. McNutt, R. Bilham, K. H. Jacob, *Science* **222**, 322 (1983); J. Beavan, R. Bilham, K. Hurst, *J. Geophys. Res.* **89**, 4478 (1984).
11. J. C. Lahr and G. Plafker, *Geology* **8**, 483 (1980); T. R. Bruns, *ibid.* **11**, 718 (1983).
12. O. J. Perez and K. H. Jacob, *J. Geophys. Res.* **85**, 7141 (Figure 4a) (1980).
13. C. D. Stephens, K. A. Fogelman, J. C. Lahr, R. A. Page, *Geology* **12**, 373 (1984).
14. P. Tapponnier and P. Molnar, *Nature (London)* **264**, 319 (1976).
15. L. R. Sykes, J. B. Kisslinger, L. House, J. N. Davies, K. H. Jacob, in *Proceedings of the Fourth Ewing Symposium* (American Geophysical Union, Washington, DC, 1981), pp. 73–79.
16. H. Kanamori, *J. Geophys. Res.* **82**, 2981 (1977).


5 August 1985; accepted 16 October 1985

# Translocation of Protein Kinase C Activity May Mediate Hippocampal Long-Term Potentiation

RAYMOND F. AKERS, DAVID M. LOVINGER, PATRICIA A. COLLEY, DAVID J. LINDEN, ARYEH ROUTTENBERG*

**Protein kinase C activity in rat hippocampal membranes and cytosol was determined 1 minute and 1 hour after induction of the synaptic plasticity of long-term potentiation. At 1 hour after long-term potentiation, but not at 1 minute, protein kinase C activity was increased twofold in membranes and decreased proportionately in cytosol, suggesting translocation of the activity. This time-dependent redistribution of enzyme activity was directly related to the persistence of synaptic plasticity, suggesting a novel mechanism regulating the strength of synaptic transmission.**

PROTEIN KINASE ACTIVATION LEADing to phosphorylation of neural proteins appears to occupy a pivotal role in the development and expression of synaptic plasticity (*1*). We have suggested that the activation of $Ca^{2+}$-phospholipid–dependent protein kinase C (PKC) and the phosphorylation of one of its substrates, protein F1, represents a key step in the expression of synaptic plasticity (*2*). This proposal is based on evidence that long-term potentiation (LTP), a persistent enhancement of hippocampal synaptic efficacy, elevates the in vitro phosphorylation of protein F1 (*3*), a 47K, synaptically enriched phosphoprotein (*p*I, 4.5) (*4*). This increase in F1 phosphorylation persisted for 3 days after the induction of LTP and was directly related to the persistence of the change in synaptic efficacy (*5*).

Since protein F1 is a PKC substrate (*6, 7*), LTP could activate PKC in vivo (*6*). Protein kinase C is activated in vitro by phosphatidylserine and diacylglycerol in the presence of $Ca^{2+}$ (*8*). However, due to the rapid breakdown of diacylglycerol after receptor activation (*9*), it is unlikely that diacylglycerol formation could account for a more prolonged activation of PKC, as would be required to maintain the long-term elevation of protein F1 phosphorylation after LTP. This prolonged activation might result from a redistribution of PKC from cytosol to membranes, similar to the strong attachment of PKC to membranes produced by the tumor-promoting phorbol esters (*10, 11*). Such a stable attachment could account for an extended period of enzyme activation necessary for the maintenance of elevated F1 phosphorylation levels during long-term plasticity. Accordingly, we determined whether the synaptic plasticity of LTP would result in the translocation of PKC activity to membranes.

Male albino rats were anesthetized with urethane and stimulating electrodes were placed in the perforant path, the axonal system that connects the entorhinal cortex with the dentate gyrus. A single recording electrode was placed in several different dorsal hippocampal positions to define the extent of synaptic invasion elicited by perfor-

Cresap Neuroscience Laboratory, Northwestern University, Evanston, IL 60201.

*To whom correspondence should be addressed.